

# INFLUENCE OF THE SCATTERING PHASE FUNCTION APPROXIMATION ON THE OPTICAL PROPERTIES OF BLOOD DETERMINED FROM THE INTEGRATING SPHERE MEASUREMENTS

A. N. Yaroslavsky,<sup>†</sup> I. V. Yaroslavsky,<sup>†</sup> T. Goldbach,<sup>‡</sup> and H.-J. Schwarzmaier<sup>\*</sup>

<sup>†</sup>Louisiana State University Medical Center, Department of Molecular and Cellular Physiology, 1501 Kings Highway, P.O. Box 33932, Shreveport, Louisiana 71130-3932; <sup>‡</sup>Heinrich-Heine University, Department of Laser Medicine, Universitätsstrasse 1, D-40225 Düsseldorf, Germany;

<sup>\*</sup>German National Research Center for Information Technology, Schloss Birlinghoven, D-53754 St. Augustin, Germany

(Paper ODB-002 received Jan. 20, 1998; revised manuscript received Nov. 13, 1998; accepted for publication Dec. 4, 1998.)

## ABSTRACT

We investigated the impact of the scattering phase function approximation on the optical properties of whole human blood determined from integrating sphere measurements using an inverse Monte Carlo technique. The diffuse reflectance  $R_d$  and the total transmittance  $T_t$  ( $\lambda = 633$  nm) of whole blood samples (Hct=38%) were measured with double-integrating sphere equipment. The scattering phase functions of highly diluted blood samples (Hct=0.1%) were measured using a goniophotometer. We approximated the experimentally determined scattering phase functions with either Henyey–Greenstein (HGPF), Gegenbauer kernel (GKPF), or Mie (MPF) phase functions to preset the anisotropy factor  $\bar{\mu}$  for the inverse problem. We have employed HGPF, GKPF, and MPF approximations in the inverse Monte Carlo procedure to derive the absorption coefficient  $\mu_a$  and the scattering coefficient  $\mu_s$ . To evaluate the obtained data, we calculated the angular distributions of scattered light for optically thick samples and compared the results with goniophotometric measurements. The data presented in this study demonstrate that the employed approximation of the scattering phase function can have a substantial impact on the derived values of  $\mu_s$  and  $\bar{\mu}$ , while  $\mu_a$  and the reduced scattering coefficient  $\mu'_s$  are much less sensitive to the exact form of the scattering phase function.

© 1999 Society of Photo-Optical Instrumentation Engineers. [S1083-3668(99)01901-2]

**Keywords** blood; integrating sphere; phase function approximation; inverse Monte Carlo technique.

## 1 INTRODUCTION

Development of new optical methods in medicine, for example, laser-induced interstitial thermo-therapy (LITT),<sup>1</sup> photodynamic therapy,<sup>2</sup> optical tomography,<sup>3</sup> or optical biopsy,<sup>4</sup> requires the knowledge of the optical properties of human tissues. Since most human tissues contain blood, the latter is an important object of investigation. Light propagation in opaque tissues is determined by their intrinsic optical properties. Those are the absorption coefficient  $\mu_a$ , the scattering coefficient  $\mu_s$ , and the scattering phase function  $f(\mu)$ , where  $\mu$

is the cosine of the scattering angle. The scattering phase function is often characterized by its average cosine  $\bar{\mu}$ , also referred to as the anisotropy factor.

Direct measurements of the optical properties of blood, such as measurements of scattering phase function, require use of optically thin samples.<sup>5,6</sup> Indirect methods may be used as an alternative to direct methods. Indirect techniques are not limited to thin samples, but require a model of light propagation in the tissue. The most widely used models are diffusion approximation,<sup>7–12</sup> numerical solutions of the transport equation,<sup>13,14</sup> and the Monte Carlo technique (MC).<sup>15,16</sup> The first two models include simplifying assumptions regarding the geometry of the experiments. In addition, they impose restrictions on the range where the optical properties can be determined. The inverse Monte Carlo technique (IMC) is not limited (at least theoretic-

When this work was done all authors were with the Department of Laser Medicine, Heinrich-Heine University, Universitätsstr. 1, D-40225 Düsseldorf, Germany. A. N. Yaroslavsky and I. V. Yaroslavsky are on leave from the Department of Optics, Saratov State University, Astrakhanskaya 83, 410071 Saratov, Russia.

Address all correspondence to A. N. Yaroslavsky. Tel: (318) 675-7359; Fax: (318) 675-6005; E-Mail: iyaros@lsumc.edu

cally) with respect to the geometrical configuration and the range of the determined optical properties, but requires comparatively long calculation times.

One of the indirect methods to determine optical properties of tissues *in vitro* is the integrating sphere technique. Diffuse reflectance  $R_d$ , total transmittance  $T_t$ , and collimated transmittance  $T_c$  are measured. Absorption coefficient  $\mu_a$ , scattering coefficient  $\mu_s$ , and anisotropy factor  $\bar{\mu}$  can be obtained from these data using an inverse method based on the radiative transfer theory. When the scattering phase function  $f(\mu)$  is available,  $\bar{\mu}$  can be readily calculated. In this case, for the determination of  $\mu_a$  and  $\mu_s$  it is sufficient to measure  $R_d$  and  $T_t$  only.

Sophisticated inverse techniques (such as adding-doubling and Monte Carlo methods) require *a priori* information about the form of the scattering phase function. An apparent possibility is to use the experimental phase function measured in an optically thin slab at a finite number of points using a goniophotometer and to employ an interpolation technique.<sup>17</sup> However, blood is an example of turbid medium with highly anisotropic scattering phase function ( $\bar{\mu} \sim 0.970-0.999$ ). For media with high anisotropy factors, precise measurements of the scattering phase function in the total angular interval ( $0^\circ-180^\circ$ ) is a difficult technical task demanding an extremely large dynamic range of measuring equipment. In addition, measurements at angles close to  $90^\circ$  are strongly affected by scattering of higher orders even for a moderate optical thickness of the sample.<sup>18</sup> Therefore, it is highly desirable to have an appropriate analytical approximation, which can be used with inverse techniques. Theoretical considerations<sup>19</sup> show that the accurate description of the scattering phase function is especially important for media with a high ( $> 0.95$ ) anisotropy factor.

Several approximations for the scattering phase function of blood are currently used: (i) The Mie scattering phase function<sup>20</sup> (MPF):

$$f_{\text{Mie}}(\theta) = \frac{S_1 S_1^* + S_2 S_2^*}{2\pi \int_0^\pi [S_1 S_1^* + S_2 S_2^*] \sin \theta d\theta'} \quad (1)$$

where

$$S_1(\theta) = \sum_{n=1}^{\infty} \frac{2n+1}{n(n+1)} \left\{ a_n \frac{P_n^1(\cos \theta)}{\sin \theta} + b_n \frac{d}{d\theta} P_n^1(\cos \theta) \right\},$$

$$S_2(\theta) = \sum_{n=1}^{\infty} \frac{2n+1}{n(n+1)} \left\{ b_n \frac{P_n^1(\cos \theta)}{\sin \theta} + a_n \frac{d}{d\theta} P_n^1(\cos \theta) \right\}. \quad (2)$$

$P_n^1(\cos \theta)$  are the associated Legendre functions, and  $a_n$  and  $b_n$  are the coefficients of the Mie series (which depend on the wavelength  $\lambda$ , the size, and the relative refractive index  $n'$  of the scatters). (ii) The Henyey-Greenstein phase function<sup>9,21,22</sup> (HGPF):

$$f_{\text{HG}}(\theta) = 4\pi^{-1}(1-g^2)[1+g^2-2g \cos(\theta)]^{-3/2},$$

$$|g| \leq 1, \quad (3)$$

and (iii) the Gegenbauer kernel phase function<sup>23</sup> (GKPF):

$$f_{\text{Gk}}(\theta) = K[1+g^2-2g \cos(\theta)]^{-(\alpha+1)}, \quad (4)$$

where

$$K = \alpha g \pi^{-1}(1-g^2)^{2\alpha} [(1+g)^{2\alpha} - (1-g)^{2\alpha}]^{-1},$$

$$\alpha > -1/2, \quad |g| \leq 1. \quad (5)$$

Thus, the Henyey-Greenstein phase function is a special case of the Gegenbauer kernel phase function with  $\alpha = 1/2$ .

In this study we analyzed the influence of the scattering phase function approximation on the resulting estimates of the optical properties of blood in the case when the experimental phase function is available for a limited range of angles. We measured the diffuse reflectance and the total transmittance at a wavelength of 633 nm of the whole blood samples with double-integrating sphere equipment and the scattering phase functions of the highly diluted blood samples with a goniophotometer. We approximated the experimental scattering phase function with either Mie, Gegenbauer kernel, or Henyey-Greenstein phase functions to preset the anisotropy factor  $\bar{\mu}$  for the inverse problem. We have employed HGPF, GKPF, and MPF approximations in the inverse Monte Carlo procedure to derive the absorption coefficient  $\mu_a$  and the scattering coefficient  $\mu_s$  of the whole blood. To investigate the accuracy of the employed phase function approximations, we calculated angular distributions of scattered light using angle-resolved MC simulations and compared the results with goniophotometric measurements of the optically thick whole blood samples.

## 2 MATERIALS AND METHODS

### 2.1 SAMPLE PREPARATION

Fresh human blood samples were obtained from healthy volunteers. Blood was collected in heparinized containers. For the measurements, we used calibrated cuvettes (thicknesses 0.01 and 0.1 mm, cuvette inner diameter 15 mm, slab geometry). Clinical tests of blood samples were performed prior to the optical measurements. All investigated samples had a hematocrit of 38% and were oxygenated up to at least 98%. The oxygenation level was controlled using a conventional blood gas analyzer

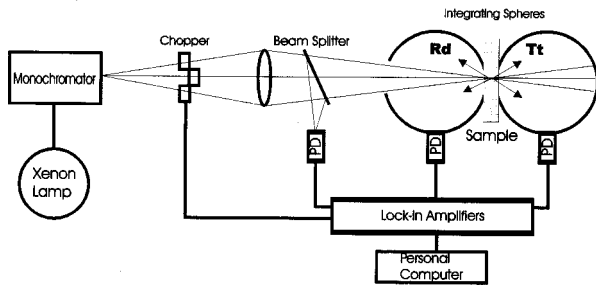


**Fig. 1** Schematics of the double-integrating sphere equipment.

(BGS 288, Ciba Corning Diagnostics Corp.). The procedure of sample preparation was performed within 2–3 min. Duration of the experiments with any particular blood sample never exceeded 3 min, to ensure that sedimentation did not obscure the results. Light microscopy was used to check that no significant hemolysis and aggregation had occurred. The pH of the samples was maintained at 7.4.

**2.2 METHODS**

**2.2.1 Integrating Sphere Measurements**

The total transmittance and the diffuse reflectance were measured at the wavelength 633 nm using a double integrating sphere system.<sup>24</sup> We used a xenon lamp (OSRAM XBO75W/2, Germany) combined with a grating monochromator (AMKO, Germany) as a light source. The beam was chopped with the frequency of 170 Hz and projected onto the sample positioned between two integrating spheres (Labsphere Inc.). The transmitted and the diffusely reflected light was registered by sandwich Si/Ge photodiodes (K1713-03, Hamamatsu, Japan). The signals were analog-to-digital (A/D) converted and measured using lock-in amplifiers (3981, ITHACO). The data were collected by a PC and stored on the hard disk. The schematic of the double-integrating sphere equipment is presented in Figure 1.

An inverse Monte Carlo method<sup>16</sup> was used to determine the optical properties of the samples from the measured quantities. The flow chart of the inverse algorithm is shown in Figure 2. The Monte Carlo technique allowed us to take into account the three-layer structure of the object (glass–blood–glass) and losses of light at the edges of the sample. The MC technique was incorporated as a forward procedure into the quasi-Newton inverse algorithm. The inverse algorithm employed the Broyden update formula to reduce the number of the forward model calls and the “trust region” approach to achieve proximity of the solution even when the initial approximation was poor.<sup>25</sup> The inverse technique allowed determination of absorption and scattering coefficients from measurements of the total transmittance and diffuse reflectance, while parameters of the phase function were preset. We used the value of  $\bar{\mu}$  obtained from the goni-

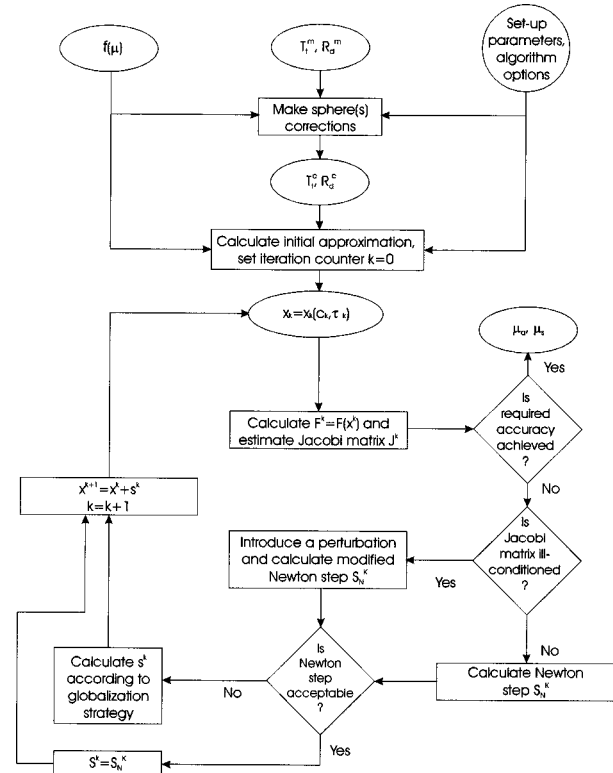


**Fig. 2** Flow chart of the quasi-Newton inverse algorithm combined with the Monte Carlo technique used to derive the optical properties from the integrating sphere measurements.  $T_i^m$  and  $R_d^m$ , measured values of the total transmittance and the diffuse reflectance.  $T_i^c$  and  $R_d^c$ , corrected values of the total transmittance and the diffuse reflectance.  $\mathbf{x} = (x_1, x_2)$ , where  $x_1 = \arcsin(c)^{1/4}$ ,  $x_2 = \tau$ ,  $c = \mu_s / \mu_t$  is the albedo,  $\tau = \mu_t d_s$  is the optical thickness of the sample,  $\mu_t = \mu_a + \mu_s$ , and  $d_s$  is the thickness of the sample.  $\mathbf{F} = (F_1, F_2)$ , where  $F_1(x^k) = T_i^c(c^k, \tau^k)$  and  $F_2(x^k) = R_d^c(c^k, \tau^k)$ .  $T_i^c$ , calculated value of the total transmittance;  $R_d^c$ , calculated value of the diffuse reflectance.

photometric measurements of the optically thin samples of whole human blood, assuming HGPF, GKPF, or MPF in the inverse algorithm (the procedure is described below).

**2.2.2 Goniophotometry**

Measurements of the angular distribution of the scattered light were performed using a He–Ne laser (wavelength 632.8 nm, cw output 10 mW, model 05-LHR-151, Melles–Griot). The cuvettes containing the blood samples were submerged in a tank filled with saline solution in order to reduce the refractive index mismatch. The scattered light was registered by a photomultiplier tube [model 4463(79-09), RCA, U.K.]. The distance between the sample and the detector was 500 mm that corresponded to the collecting angle of the detector  $\sim 0.65^\circ$ . The data were A/D converted and acquired by a computer. The experimental arrangement for measuring the angular distribution of the scattered light is presented in Figure 3.

To determine the anisotropy factor of blood, scattering phase functions were measured. For these

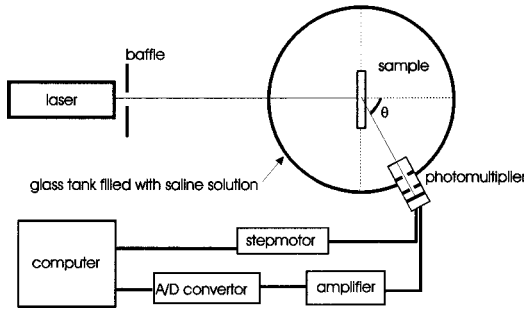


**Fig. 3** Schematics of the goniophotometer.

experiments we used human whole blood diluted to a hematocrit of 0.1% with a phosphate buffer solution (*pH* 7.4). The measurements were performed in the range from 2° to 18° with the stepwidth of 1° counting from the direction of the incident beam. The upper limit of the angular range was determined by the dynamic range of the detector. We used a 0.01 mm cuvette to ensure a single scattering regime. The experimental data were fitted with HGPF, GKPF, and MPF. The target function for the minimization procedure was

$$\sum_{i=0}^N [Af^c(\theta_i) - f^e(\theta_i)]^2 \rightarrow \min, \quad (6)$$

where *A* is the optimized normalization factor, *f<sup>c</sup>(θ<sub>i</sub>)* is the assumed scattering phase functions, and *f<sup>e</sup>(θ<sub>i</sub>)* is the measured scattering phase function corrected for the refractive index mismatch at the sample interfaces.

To verify the accuracy of the used approximations we measured the angular distribution of light scattered by whole blood samples with a hematocrit of 38% and thickness of 0.1 mm. In this case, multiple scattering dominated due to the large optical depth of the samples. The measurements were performed in the range from 2° to 156° with a step of 2° counting from the direction of the incident beam. The angular distribution of light scattered by optically thick samples was calculated with angle-resolved Monte Carlo (AMC) simulations alternatively using different phase function approximations and the respective values of *μ<sub>a</sub>* and *μ<sub>s</sub>* determined by the inverse Monte Carlo method from the double-integrating sphere measurements. The calculated scattered light distributions were compared with the measured ones. To achieve angular resolution we modified the basic Monte Carlo algorithm<sup>26,27</sup> in the following way. The total range of the scattering angles was divided in *N* intervals. The number of photons leaving the sample at the angles within *i*th interval (*i*=1,...,*N*) was estimated in the course of the simulations. The scattered light intensity registered by the detector was calculated using the formula

$$I_i = N_{\text{phs}} / [M |\cos(\theta_i - \Delta\theta/2) - \cos(\theta_i + \Delta\theta/2)|], \quad (7)$$

where *I<sub>i</sub>* is the normalized intensity at the angle *θ<sub>i</sub>* (the number of photons per unit of the solid angle), and *N<sub>phs</sub>* is the number of photons exiting the sample within the angle interval [*θ<sub>i</sub>*−*Δθ*/2, *θ<sub>i</sub>*+*Δθ*/2]. *M* is the total number of the launched photons.

For the Henyey–Greenstein distribution, the random values of the cosine of the scattering angle during the AMC simulation were obtained using the formula<sup>26</sup>

$$\mu_{\text{srd}} = [1 + g^2 - \{(1 - g^2) / (1 - g + 2g\eta)\}^2] / 2g, \quad (8)$$

and for the case of the Gegenbauer kernel phase function using the formula

$$\mu_{\text{srd}} = (1 + g^2 - 1/\sqrt{\xi_{\text{srd}}}) / 2g, \quad (9)$$

where  $\xi_{\text{srd}} = 2\alpha g \eta / K + (1 + g)^{-2\alpha}$ , *μ<sub>srd</sub>* is the cosine of the scattering angle, and *η* is a random number uniformly distributed in the interval (0; 1). Setting *α* equal to 1/2 in formula (9) reduces it to formula (8).

In the case of the MPF, the random value of the scattering angle was determined using the numeric algorithm similar to the one described in Ref. 28.

### 3 RESULTS

Seven samples of whole blood [Hct=38%, oxygen saturation (OS) >98%] were measured at *λ* = 633 nm with the double-integrating sphere equipment. The optical properties obtained from the measurements of the diffuse reflectance and the total transmittance using the inverse Monte Carlo procedure are summarized in Table 1. These optical properties were derived using HGPF, GKPF, and MPF approximations for the scattering phase function. The refractive index of the blood samples was assumed to be 1.38. For the refractive index of the cuvette walls the value of 1.46 was accepted. The anisotropy factors were determined from goniophotometric measurements. The values of the anisotropy factor were calculated for each phase function approximation.

An example of the direct measurement of the scattering phase function at 633 nm using a diluted blood sample is shown in Figure 4. The results of the best fit using HGPF, GKPF, and MPF are also presented. For the Henyey–Greenstein phase function the least-squares procedure resulted in *μ* = 0.971, for the Gegenbauer kernel phase function *μ* = 0.997 (*g* = 0.891, *α* = 3.658), and for the Mie scattering phase function *μ* = 0.996, which corresponded to the scatters with a radius of 2.995 *μm* and refractive index of 1.04 relative to the phosphate buffer solution.

**Table 1** Optical properties of human whole blood at 633 nm, determined from integrating sphere measurements assuming either the Henyey–Greenstein, Gegenbauer kernel, or Mie phase function (standard error of the Monte Carlo simulation 0.5%), with the values of anisotropy factor obtained from goniophotometry.

Optical properties	Henyey–Greenstein phase function	Gegenbauer kernel Phase function	Mie phase function
$\bar{\mu}$	$0.971 \pm 0.001$	$0.9970 \pm 0.0001$	$0.9962 \pm 0.0001$
$\mu_a$ ( $\text{mm}^{-1}$ )	$1.52 \pm 0.06$	$1.61 \pm 0.06$	$1.63 \pm 0.05$
$\mu_s$ ( $\text{mm}^{-1}$ )	$40 \pm 3$	$413 \pm 17$	$239 \pm 16$
$\mu'_s$ ( $\text{mm}^{-1}$ )	$1.17 \pm 0.12$	$1.24 \pm 0.09$	$0.91 \pm 0.08$

The measured angular distribution of light scattered by a 0.1 mm thick sample of the whole blood (Hct=38%) is presented in Figure 5(a). The graph also features the scattered light distributions obtained from AMC simulations using the above-mentioned approximations for the scattering phase function with the optical properties from Table 1. To quantify the accuracy of the employed scattering phase function approximations, we calculated the residuals at each angular point. The residuals were defined as differences between the calculated and measured intensities of the scattered light, normalized on the measured values. The residuals are presented in Figure 5(b).

the HGPF and GKPF are nearly the same, while the reduced scattering coefficient when using the MPF is significantly lower. It appears that there are two main reasons for the discrepancies in the deduced optical properties. First, fitting of the experimental phase function in a limited angular interval with different approximations leads to different estimations of  $\bar{\mu}$  (see Table 1). This is caused by imposing an assumed behavior of the phase function in the range of angles where no experimental information is available. Second, media with the same values of  $(\mu_a, \mu_s, \bar{\mu})$  but different phase functions may ex-

### 4 DISCUSSION

The results of the study show that there are essential discrepancies in the optical properties obtained using either Henyey–Greenstein, Gegenbauer kernel, or Mie approximations of the scattering phase function (see Table 1). The differences in the absorption coefficients are not substantial, while the values of the scattering coefficients and the anisotropy factors differ considerably. The reduced scattering coefficients calculated using the values of the optical properties determined in the assumption of

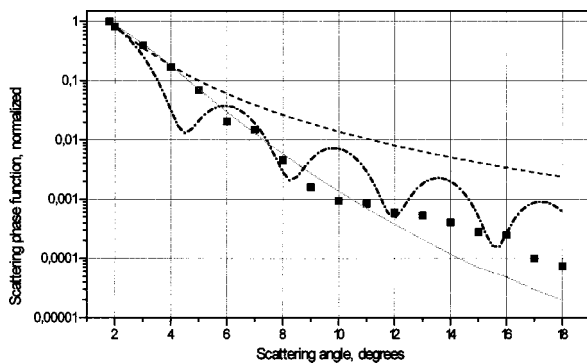


**Fig. 4** Scattering phase function of blood at the wavelength of 633 nm. Squares—measured data (blood sample Hct=0.1%, OS>98% in 0.01 mm cuvette); dash line—best fit with HGPF ( $\bar{\mu} = 0.971$ ); solid line—best fit with GKPF ( $\bar{\mu} = 0.997$ ); and dash and dot line—best fit with MPF ( $\bar{\mu} = 0.996$ ).

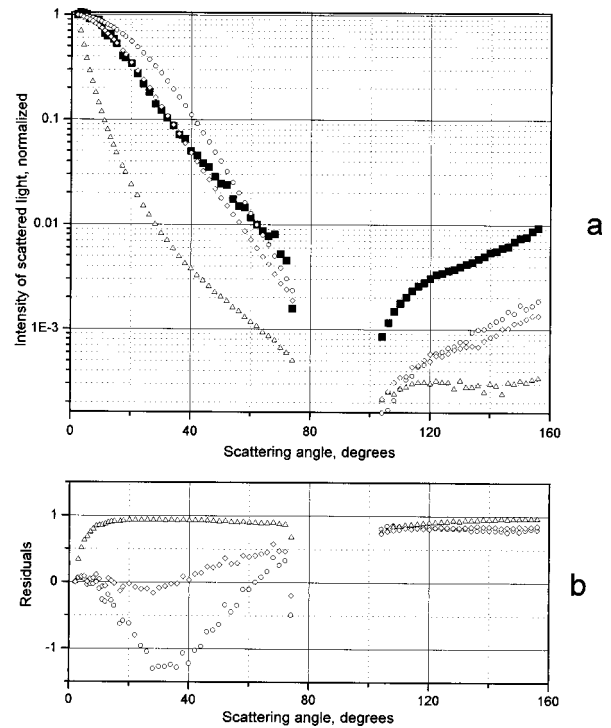


**Fig. 5** (a) Angular distribution of light scattered by the 0.1 mm thick sample of whole blood (Hct=38%) at the wavelength of 633 nm. Solid squares—measured; open circles—AMC simulation using the Gegenbauer kernel phase function; open triangles—AMC simulation using the Henyey–Greenstein phase function; open diamonds—AMC simulation using the Mie phase function. (b) Residuals of the calculated curves.

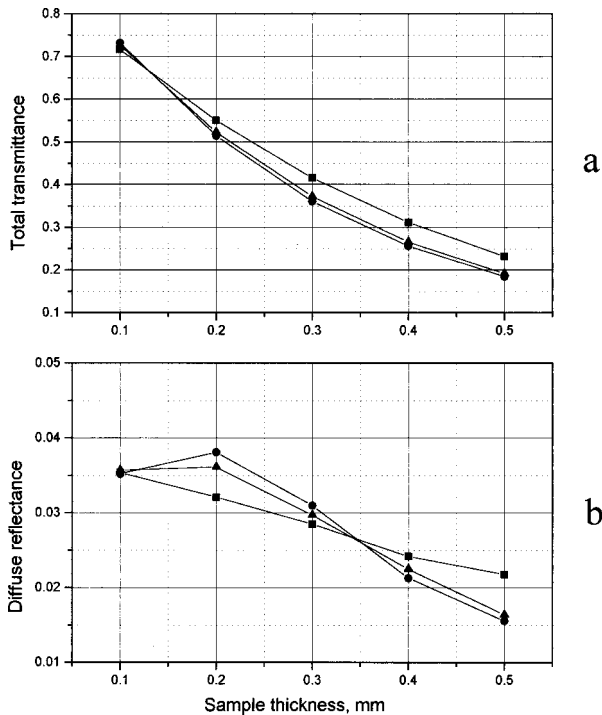


**Fig. 6** Total transmittance and diffuse reflectance as functions of the sample thickness for the three approximations of the phase function as calculated by the Monte Carlo method (attenuation coefficient: 240.6/mm, albedo: 0.99, refractive index: 1.38). Squares, the Henyey–Greenstein phase function ( $g=0.996$ ); circles, the Gegenbauer kernel phase function ( $g=0.865$ ,  $\alpha=3.658$ ); and triangles, the Mie phase function (s.r.=2.995  $\mu\text{m}$ ,  $n_{\text{rel}}=1.04$ ). The anisotropy factor for all phase functions is 0.996. (a) Total transmittance and (b) diffuse reflectance.

hibit substantially different integrating sphere responses (i.e.,  $R_d$  and  $T_t$ ). This suggests that besides  $\bar{\mu}$ , the higher moments of the scattering phase function may play a role in the formation of the intensity distribution. In order to verify the last statement, we have performed a series of forward Monte Carlo simulations assuming a fixed set of the optical properties ( $\mu_a, \mu_s, \bar{\mu}$ ), but different phase functions. An example of these simulations is presented in Figure 6. The total transmittance and the diffuse reflectance as functions of the sample thickness were calculated using HGPF, GKPF, and MPF approximations for the scattering phase function. For these simulations we used the same value of the anisotropy factor for all phase function approximations ( $\bar{\mu}=0.996$ ). The geometry of the simulation

corresponded to the geometry of our experimental setup. It is clearly seen that both  $R_d$  and  $T_t$  are strongly affected by the form of the phase function, and that the magnitude of this influence depends on the thickness of the sample. It should be noted that with further growth of the sample thickness the diffuse reflectance eventually reaches its saturation value (not shown in Figure 6), which still may be different for the different phase functions.

Below we present a comparison of the data determined for the oxygenated blood in this study with the data on the optical properties of the whole blood available in the literature. Flock et al.<sup>5</sup> performed measurements of the total attenuation coefficient of the diluted blood samples. Roggan et al.<sup>29</sup> investigated the optical properties of whole human blood under flow conditions. To compare these data with the data presented in this study, we have calculated extinction efficiency factors using formulas from Ref. 30. We have used the value of 112.5  $\mu\text{m}^3$  for the erythrocyte volume and 28.17  $\mu\text{m}^2$  for its geometrical cross section in the recalculation. For the HGPF we obtained  $Q_t \approx 0.44$ , for the GKPF  $Q_t \approx 4.35$ , and for the MPF  $Q_t \approx 2.53$ . The best agreement with the result from Ref. 5,  $Q_t \approx 3.05$ , has been achieved when the Mie phase function was assumed. The comparison with the values obtained in Ref. 29, for the completely oxygenated whole blood (Hct=5%,  $\pi=300$  mosmol/L,  $\gamma=500$  s<sup>-1</sup>), is presented in Table 2. The agreement in the absorption efficiency factors determined in Ref. 29 and in our work for all three phase functions investigated can be considered as excellent, while for the scattering efficiency factor the best agreement is again achieved in assumption of the Mie scattering phase function. It should be mentioned that we assume a linear increase of absorption and scattering with increase of hematocrit, whereas the dependence of the scattering coefficient on the hematocrit may be more complicated in reality.

The comparison of the optical constants obtained from integrating sphere measurements using different phase function approximations clearly shows (see Table 1) that the scattering coefficient is highly sensitive to the shape of the phase function. Among the three investigated phase functions, the Mie approximation seems to provide the best description of the measured data (see Figure 5), although we accounted neither for polydispersity nor for nonsphericity of the red blood cells. Taking into consid-

**Table 2** Absorption efficiency factor  $Q_a$  and scattering efficiency factor  $Q_s$  at the wavelength of 633 nm, obtained in this work and recalculated from Ref. 29.

	Henyey–Greenstein phase function	Gegenbauer kernel phase function	Mie phase function	Ref. 29
$Q_a$	0.016	0.016	0.017	0.016
$Q_s$	0.42	4.34	2.51	2.56

eration these factors will further improve the accuracy of the model. This means that if the precise data on the scattering coefficient of blood are of interest, the Mie phase function should be used despite the increased computational costs. At the same time transport parameters (the absorption coefficient and the reduced scattering coefficient) are considerably less influenced by the errors in the assumed phase function.

## REFERENCES

1. *Laser-induced Interstitial Thermo-therapy*, G. Müller and A. Roggan, Eds., Vol. PM25, SPIE Press, Bellingham, WA (1995).
2. J. J. Schuitmaker, P. Baas, H. L. van Leengoed, F. W. van der Meulen, W. M. Star, and N. van Zandwijk, "Photodynamic therapy: A promising new modality for the treatment of cancer," *J. Photochem. Photobiol., B* **34**, 3–12 (1996).
3. *Optical Tomography, Photon Migration and Model Media: Theory, Human Studies, and Instrumentation*, B. Chance and R. Alfano, Eds., *Proc. SPIE* **2389** (1995).
4. R. Richards-Kortum and E. Sevick-Muraca, "Quantitative optical spectroscopy for diagnostics," *Annu. Rev. Phys. Chem.* **47**, 555–606 (1996).
5. S. T. Flock, B. C. Wilson, and M. S. Patterson, "Total attenuation coefficient and scattering phase function of tissues and phantom materials at 633 nm," *Med. Phys.* **14**, 835–841 (1987).
6. R. J. Zdrojkowski and R. L. Longini, "Optical transmission through whole blood illuminated with high collimated light," *J. Opt. Soc. Am.* **59**, 898–903 (1969).
7. J. M. Steinke and A. P. Shephard, "Diffusion model of the optical absorbance of whole blood," *J. Opt. Soc. Am. A* **5**, 813–822 (1988).
8. L. Reynolds, "Optical diffuse reflectance and transmittance from anisotropically finite blood medium," PhD dissertation, Electrical Engineering Department, University of Washington, Seattle, WA (1975).
9. J. M. Steinke and A. P. Shepherd, "Diffuse reflectance of whole blood: Model for a diverging light beam," *IEEE Trans. Biomed. Eng.* **BME-34**, 826–834 (1987).
10. R. J. Zdrojkowski and N. R. Pisharoty, "Optical transmission and reflection by blood," *IEEE Trans. Biomed. Eng.* **BME-17**, 122–128 (1970).
11. C. C. Johnson, "Optical diffusion in blood," *IEEE Trans. Biomed. Eng.* **BME-17**, 129–133 (1970).
12. R. L. Longini and R. Zdrojkowski, "A note on the theory of backscattering of light by living tissue," *IEEE Trans. Biomed. Eng.* **BME-15**, 4–10 (1968).
13. M. C. van de Hulst, *Multiple Light Scattering*, Academic, New York (1980).
14. G. D. Pedersen, N. J. McCormick, and L. O. Reynolds, "Transport calculations for light scattering in blood," *Biophys. J.* **16**, 199–207 (1976).
15. A. Roggan, O. Minet, C. Schröder, and G. J. Müller, "Determination of optical tissue properties with double integrating sphere technique and Monte Carlo simulations," *Proc. SPIE* **2100**, 42–56 (1994).
16. I. V. Yaroslavsky, A. N. Yaroslavsky, T. Goldbach, and H.-J. Schwarzmaier, "Inverse hybrid technique for the determination of the optical properties of turbid media," *Appl. Opt.* **35**, 6797–6809 (1996).
17. P. van der Zee, "Methods for measuring the optical properties of tissue samples in the visible and near infrared wavelength range," in *Medical Optical Tomography: Functional Imaging and Monitoring*, G. Müller, B. Chance, et al., Eds., *SPIE Soc. Photo-Opt. Instrum. Eng. Inst. Ser.* **11**, 166–192 (1993).
18. N. G. Khlebtsov, "Role of multiple scattering in turbidimetric investigations of dispersed systems," *J. Appl. Spectrosc.* **40**, 243–247 (1984).
19. H. C. van de Hulst, *Multiple Light Scattering*, Vol. 2, p. 488, Academic, New York (1980).
20. L. Reynolds, C. Johnson, and A. Ishimaru, "Diffuse reflectance from a finite blood medium: Applications to the modeling of fiber optic catheters," *Appl. Opt.* **15**, 2059–2067 (1976).
21. W. F. Cheong, S. A. Prah, and A. J. Welch, "A review of the optical properties of biological tissues," *IEEE J. Quantum Electron.* **26**, 2166–2185 (1990).
22. G. D. Pedersen, N. J. McCormick, and L. O. Reynolds, "Transport calculations for light scattering in blood," *Biophys. J.* **16**, 199–207 (1976).
23. L. O. Reynolds and N. J. McCormick, "Approximate two-parameter phase function for light scattering," *J. Opt. Soc. Am.* **70**, 1206–1212 (1980).
24. A. Roggan, K. Dörschel, O. Minet, D. Wolf, and G. Müller, "The optical properties of biological tissue in the near infrared spectral range—review and measurements," in *Laser-induced Interstitial Thermo-therapy*, G. Müller and A. Roggan, Eds., Vol. PM25, pp. 10–45, SPIE Press, Bellingham, WA (1995).
25. J. E. Dennis, Jr. and R. B. Schnabel, *Numerical Methods for Unconstrained Optimization and Nonlinear Equations*, Prentice-Hall, Englewood Cliffs, NJ (1983).
26. M. Keijzer, S. L. Jacques, S. A. Prah, and A. J. Welch, "Light distribution in artery tissue: Monte Carlo simulations for finite diameter laser beams," *Lasers Surg. Med.* **9**, 148–154 (1989).
27. I. V. Yaroslavsky and V. V. Tuchin, "Light propagation in multilayer scattering media: Modeling by the Monte Carlo method," *Opt. Spectrosc.* **72**, 505–509 (1992).
28. J. R. Zijp and J. J. ten Bosch, "Use of tabulated cumulative density functions to generate pseudorandom numbers obeying specific distributions for Monte Carlo simulations," *Appl. Opt.* **33**, 533–534 (1994).
29. A. Roggan, M. Friebe, K. Dörschel, A. Hahn, and G. Müller, "Optical properties of circulating human blood," *Proc. SPIE* **3195**, 51–63 (1998).
30. A. Ishimaru, *Wave Propagation and Scattering in Random Media*, Vol. 1, pp. 65 and 66, Academic, New York (1978).